

GA-A27310

ELM MITIGATION TECHNIQUES

**by
T.E. EVANS**

MAY 2012



DISCLAIMER

This report was prepared as an account of work sponsored by an agency of the United States Government. Neither the United States Government nor any agency thereof, nor any of their employees, makes any warranty, express or implied, or assumes any legal liability or responsibility for the accuracy, completeness, or usefulness of any information, apparatus, product, or process disclosed, or represents that its use would not infringe privately owned rights. Reference herein to any specific commercial product, process, or service by trade name, trademark, manufacturer, or otherwise, does not necessarily constitute or imply its endorsement, recommendation, or favoring by the United States Government or any agency thereof. The views and opinions of authors expressed herein do not necessarily state or reflect those of the United States Government or any agency thereof.

GA-A27310

ELM MITIGATION TECHNIQUES

by
T.E. EVANS

This is a preprint of a paper to be presented at the Twentieth International Conference on Plasma-Surface Interactions in Controlled Fusion Devices, May 21–25, 2012 in Aachen, Germany and to be published in the *J. Nucl. Mater.*

**Work supported by
the U.S. Department of Energy
under DE-FC02-04ER54698**

**GENERAL ATOMICS PROJECT 30200
MAY 2012**



ELM mitigation techniques

T. E. Evans^{a*}

^aGeneral Atomics, PO Box 85608, San Diego, California 92186-5608, USA

Abstract. Large edge-localized mode (ELM) control techniques must be developed to help ensure the success of burning and ignited fusion plasma devices such as tokamaks and stellarators. In full performance ITER tokamak discharges, with $Q_{DT} = 10$, the energy released by a single ELM could reach ~ 30 MJ which is expected to result in an energy density of $10\text{--}15$ MJ/m² on the divertor targets. This will exceed the estimated divertor ablation limit by a factor of 20–30. A worldwide research program is underway to develop various types of ELM control techniques in preparation for ITER H-mode plasma operations. An overview of the ELM control techniques currently being developed is discussed along with the requirements for applying these techniques to plasmas in ITER. Particular emphasis is given to the primary approaches, pellet pacing and resonant magnetic perturbation fields, currently being considered for ITER.

PACS: 28.52-s, 52.55.Fa, 52.55.Rk

1. INTRODUCTION

1.1. Overview of ITER objectives and edge-localized mode effects

In the next generation of “ITER scale” tokamaks deuterium (D) and tritium (T) fuel mixtures will be used to produce DT fusion reactions resulting in a power gain factor $Q_{DT} = P_{fusion}/P_{aux}$ of 10. In ITER, it is expected that 15 MA high confinement (H-mode) plasmas will produce sufficient alpha particle heating power $P_\alpha = P_{fusion} - P_{neutron}$ to provide 90% of the total power $P_T = P_{fusion} + P_{aux}$ required to reach $Q_{DT} = 10$ with an auxiliary heating power $P_{aux} = (1 + Q_{DT})^{-1} P_T$ assuming a P_T between 330 MW and 550 MW [1]. In plasmas with discharge lengths of 300–500 s, edge-localized modes (ELMs) are expected to periodically eject as much as 20% of the pedestal energy or between 6.3 GJ and 17.5 GJ when integrated over the duration of the discharge. This is approximately 7% of the DT energy produced during each full-length discharge. While ELM losses will have a significant negative impact on the net thermal generating efficiency of the device, a greater concern involves the interaction of the large energy impulses released by each ELM (ΔW_{ELM}) with the plasma facing surfaces (PFCs). Estimates based on scaling the energy released by large Type-I ELMs in present tokamaks [2] to “ITER scale” devices imply that in plasmas with P_T between 330 MW and 550 MW each ELM will release energies ranging from $\Delta W_{ELM} = 20$ MJ to 35 MJ. Depending on the interaction area of the ELMs with divertor and main chamber PFCs, material erosion limits require that this energy must be reduced a factor of 20–30 in order to prevent an accelerated degradation of the divertors and wall surfaces [2]. Thus, ELMs pose a significant concern for the successful development of the tokamak concept as burning plasma device and a rapidly growing worldwide program, focused on ELM control strategies, has recently become one of the most active areas of research in the magnetic fusion program.

Since the H-mode performance in tokamak plasmas increases with the core temperature and the core temperature scales with the pedestal temperature due to profile stiffness, it is necessary to maintain much higher pedestal temperatures in ITER than those in existing tokamaks. Calculations using the TGLF-09 and GLF23 codes predict that the H-mode pedestal temperature in ITER must be maintained at near 5 keV with $P_{aux} = 30$ MW and $P_{DT} = 300$ MW, assuming a pedestal density of $9 \times 10^{19} \text{ m}^{-3}$ and a density peaking factor of 1.1, in order to achieve $Q_{DT} = 10$ [3]. As discussed in Sec. 2, these pedestal parameters,

along with a series of related ITER operational requirements, place very strong constraints on the ELM mitigation systems. For example, these pedestal requirements result in an insurmountable experimental challenge for proving that an ELM control technique will work in ITER using our present devices since they require tests of the system in plasmas with pedestal temperature and density that are not attainable in any existing tokamak. In addition, it is important to demonstrate that the ITER ELM control system will work without significantly degrading the pedestal pressure required by the TGLF-09 predictions since this would jeopardize ITER's ability to reach $Q_{DT} = 10$. Proving this point will be very difficult without having pedestal plasmas equivalent to those in ITER.

1.2. *Summary of ELM control approaches*

Due to the urgency of the ELM issue for ITER-class tokamaks and beyond, a rather large array of suppression and mitigation concepts have recently emerged, including techniques such as: 1) the application of edge Resonant Magnetic Perturbation (RMP) fields [4–8], 2) ELM pacing with small, high frequency, frozen deuterium pellets [9–11], 3) operations in naturally occurring quiescent H-mode (QH-mode) plasmas [12–16] and I-mode regimes [17–19], 4) impurity seeding [20–22], 5) the use of small periodic vertical equilibrium displacements [23–25], 6) the injection of supersonic molecular beams [26–28], 7) the application of low recycling wall materials like lithium coatings [29–31], 8) the application of edge Electron Cyclotron Heating (ECH) [32], 9) the introduction of small toroidal ripple fields [33,34], and 10) operations in naturally occurring small ELM regimes which include the Enhanced D_α (EDA) H-mode [35], grassy ELMs [36,37], the High Recycling Steady (HRS) H-mode [38], Type-II ELMs [39], Type V ELMs [40] and snowflake divertor configurations [41]. While several of these approaches have emerged quite recently others such as pellet pacing, operations in QH-modes, the application of edge RMP fields and a wide variety of small ELM regimes have been developed to a relatively high level of maturity over an extended period and on a broad range of tokamaks. For example, a 2006 review on small ELM regimes [42] provides a good overview of this area of research with the exception of the more recent snowflake divertor concept [43].

Although many of these techniques hold significant promise for mitigating ELMs in ITER, the discussion in this paper is focused on the two systems that have been incorporated into the ITER baseline plan i.e., pellet pacing and edge RMP fields. As a prerequisite for the discussion of these systems, a brief summary of the requirements for

ELM suppression in ITER is given in Sec. 2. While these requirements are generally applicable for any of the proposed ITER ELM mitigation system, they are particularly important for the design of the pellet pacing and RMP ELM control systems since they must reliably mitigate and/or suppress ELMs during the initial non-nuclear phase in order to prepare for H-mode operations in the DT phase of ITER. Section 3 provides an overview of the recent results and the current status of ELM pellet pacing. This is followed, in Sec. 4, by a discussion of the status of edge RMP research and a summary in the final section.

2. REQUIREMENTS FOR ELM MITIGATION AND SUPPRESSION IN ITER

2.1. Primary ELM mitigation requirements in ITER

The requirements for ELM mitigation and suppression in ITER are relatively stringent due a variety of constraints that must be satisfied in order to meet the project objectives while ensuring the integrity of the plasma facing components over the lifetime of the machine. As shown in Fig. 1, the number of ELMs that are expected in ITER before the divertor must be replaced is a strong function of ΔW_{ELM} , the ELM energy impulse time (Δt_{ELM}) and the properties of the materials used for the divertor target plates [44]. As shown in Fig. 1, the most basic requirement for any ELM control system is to reliably reduce ΔW_{ELM} by the largest factor possible while maintaining high core density H-mode plasmas with electron pedestal collisionalities (v_e^*) of approximately 0.1–0.03 needed to obtain $Q_{\text{DT}} = 10$. Recently, data on the consequences of intense energy impulses interacting with ITER relevant divertor materials has emerged from laboratory experiments using a quasi-stationary plasma accelerator [45,46]. In these experiments, divertor target components were exposed to large transient energy impulses similar to those expected during an ELM in ITER. Results from these studies have led to a reduction of the maximum acceptable ELM impulse energy density (ε_{ELM}) in ITER to $\varepsilon_{\text{ELM}} = 0.5 \text{ MJ m}^{-2}$ assuming $\Delta t_{\text{ELM}} \geq 250\text{--}500 \mu\text{s}$ [47]. For 15 MA $Q_{\text{DT}} = 10$ plasmas, referred to as Scenario 2, inductive H-modes, with $R = 6.2 \text{ m}$, $a = 2.0 \text{ m}$, $I_p = 15 \text{ MA}$, $B_T = 5.3 \text{ T}$, an H-mode factor $H_{89(y,2)} = 1.0$, an internal inductance $l_i = 0.8$, elongation $\kappa = 1.7\text{--}1.85$, a normalized plasmas pressure $\beta_N = 1.8$ and a fusion burn duration $\tau_{\text{burn}} = 300\text{--}500 \text{ s}$ [1], this corresponds to ELMs with $\Delta W_{\text{ELM}} \sim 0.7 \text{ MJ}$ [47]. Here, it is assumed that the surface area (A_{ELM}) of the ELM interaction with the divertor targets is $A_{\text{ELM}} = 1.4 \text{ m}^2$. On the other hand, as shown in Fig. 2 [47], the acceptable level of ε_{ELM}

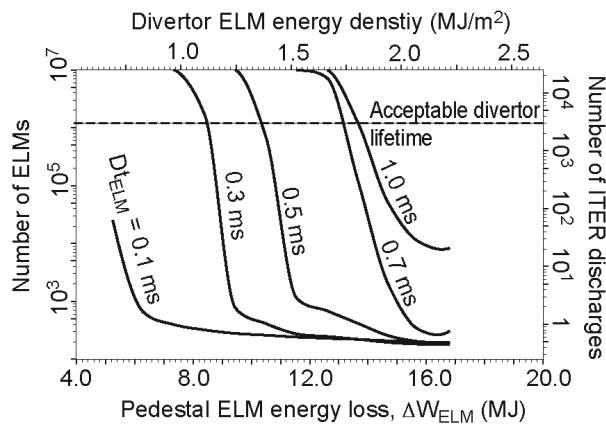


Fig. 1. Number of Type-I ELMs and full length ITER discharges resulting in the complete erosion of the tungsten divertor in ITER vs ΔW_{ELM} and the deposition time (Δt_{ELM}) of the ELM energy impulse as discussed in Federici, *et al.*, Ref. 44.

depends strongly on I_p and A_{ELM} . For tungsten divertor target plates, acceptable values of ΔW_{ELM} reside in the regions below the solid lines in Fig. 2 where $A_{\text{ss}} = 1.4 \text{ m}^2$ is the steady-state heat flux area between ELMs. As the size of the ELMs increases, it is expected that A_{ELM} will increase from A_{ss} (red solid line) to $3A_{\text{ss}}$ (blue solid line) and to $6A_{\text{ss}}$ (green solid line) however the scaling of the heat flux area with ELM size is not known at this time leading to additional uncertainty in the requirements of ΔW_{ELM} in ITER. The expectation is that the acceptable ΔW_{ELM} will increase from approximately 0.7 MJ to 2.1 MJ and then to 4.2 MJ in the $I_p = 15 \text{ MA}$ ITER Scenario 2 plasmas as the heat flux area increases from A_{ss} to $3A_{\text{ss}}$ and to $6A_{\text{ss}}$ keeping ε_{ELM} constant. A similar dependence on I_p is seen for the acceptable levels of ΔW_{ELM} on the Be walls as indicated by the dashed lines in Fig. 2.

In addition to the Scenario 2 H-mode, several advanced operating scenarios are being considered for ITER beyond the completion of the $Q_{\text{DT}} = 10$ phase [1]. Each of these imposes additional constraints on the ELM control systems. One of these is the Hybrid or Scenario 3 regime. This is envisioned to have plasmas with $I_p = 12 \text{ MA}$, $l_i = 0.9$, $\beta_N = 2.0\text{--}2.5$, $H_{98(y,2)} = 1.0\text{--}1.2$, $\tau_{\text{burn}} \geq 1000 \text{ s}$ and a noninductive I_p fraction of 0.5. It is noted that in long τ_{burn} plasmas ELM management will most likely require an ability to externally control, using an active feedback algorithm, the parameters of the mitigation/suppression system in order to adjust for changing wall and divertor conditions. In the same context, the system must be able to respond to rapid transients such as sawteeth and changes in confinement due core MHD modes. In addition, changing heating and non-inductive current drive requirements as well as transient profile changes due core fueling with high velocity, cryogenic, DT pellets must be seamlessly integrated into the ELM control feedback algorithm.

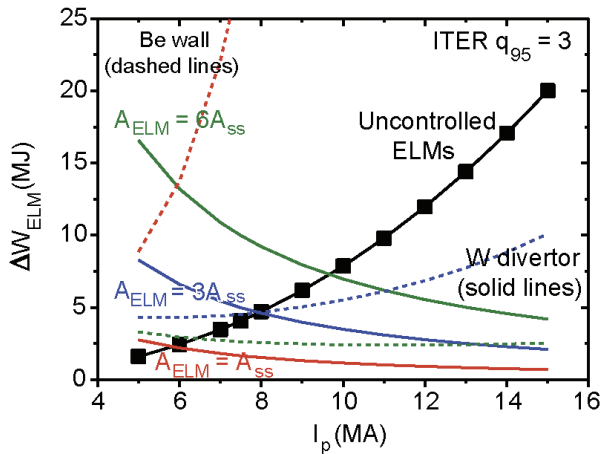


Fig. 2. Scaling of ΔW_{ELM} with the ITER plasma current in $q_{95} = 3$ discharges. The solid lines represent the upper limit for acceptable ELM energy impulses with tungsten (W) divertor plates assuming ELM surface interactions area of $A_{\text{ss}} = 1.4 \text{ m}^2$ (red), $3A_{\text{ss}}$ (blue) and $6A_{\text{ss}}$ (green). Upper limits for ΔW_{ELM} on the beryllium walls for three values of A_{ss} are shown by the dashed lines. (Figure courtesy of A. Loarte, see Ref. 47.)

2.2. Secondary ELM mitigation requirements in ITER

While the primary requirements outlined above pose a significant challenge for both of the ELM control systems presently included in the ITER baseline design, there are a variety of secondary, but no less important, requirements that must also be met. The first of these involves the ability to mitigate or suppress ELMs during I_p ramps at the beginning and end of each discharge. Since it is necessary to operate in an H-mode during both the I_p rampup and rampdown phase of each discharge, ELMs must be controlled and here again it is necessary to be able to actively adjust the ELM control system with an appropriately tuned feedback algorithm. Another critical constraint adding to this complex mix of requirements is the need to mitigate or suppress the first ELM following the H-mode transition. During this particularly sensitive phase of operations, when the safety factor and pedestal profiles are dynamically evolving, due to the I_p ramp and the change in confinement across the H-mode transition, it will be necessary to track and optimize the performance of the ELM control system in order to ensure a safe transition in the confinement without any significant ΔW_{ELM} excursions. Experience has shown that the first ELM following the H-mode transition and the associated ELM-free period results in a particularly large ΔW_{ELM} that may lead to a substantially enhanced erosion rate or melting of the tungsten divertors and the main chamber beryllium walls. Such an event, if left uncontrolled, could lead to a large impurity influx and a radiative collapse of the plasma that might induce a major disruption and jeopardize the structural integrity of the device.

It should be noted here that ITER will not have a particularly large level of toroidal rotation due to a relatively modest amount of neutral beam injected (NBI) momentum input and, if left uncontrolled large ELMs are known to transport toroidal momentum very effectively. Thus, the ELM control system must not enhance toroidal momentum transport since this could result in locked modes due to the penetration of low n,m non-axisymmetric field-errors and a subsequent termination of the discharge. Here, again it is seen that strong ELM mitigation or suppression is essential not only for reducing ΔW_{ELM} but for maintaining good toroidal momentum confinement. This issue becomes significantly more challenging in ignited plasmas when the external heating and torque from the NBI system is no longer needed to maintain burning plasma conditions. In this case any loss of toroidal momentum, due to ELMs, sawteeth, etc., will become a much more serious issue and the ELM control system will need to operate at the highest possible

level of performance in order to maintain conditions required for burning and ignited plasma operations. An associated issue is the effect of the ELM control system on energetic particles such as neutral beam ions and alpha particles. Obviously, a prompt loss of alpha particles will reduce P_α and the fusion gain while a prompt loss of energetic NBI ions will not only affect the ability to obtain H-modes but reduce the toroidal torque needed to maintain adequate levels of toroidal rotation to avoid locked modes.

A final set of requirements ranges from the ability to maintain detached target plate conditions during impurity seeded radiative divertor operations, which is required to reduce the steady-state heat flux to the divertors, to a compatibility with high throughput cryopump operations and with neoclassical tearing mode suppression by electron cyclotron current drive (ECCD). In addition, the system must be able to mitigate or suppress ELMs in helium plasmas during the non-nuclear operations phase of the machine, avoid large steady-state divertor and wall heat flux asymmetries and must be compatible with the electron cyclotron heating (ECH) and ion cyclotron resonant heating (ICRH).

3. ELM MITIGATION USING CRYOGENIC DEUTERIUM PELLETS

One of the primary strategies planned for limiting the maximum ΔW_{ELM} in ITER is based on periodically injecting cryogenic deuterium pellets at a frequency that significantly exceeds the expected natural ELM frequency $f_{\text{N_ELM}} = 1\text{--}2 \text{ Hz}$ in ITER. This is referred to as pellet pacing [9]. Using a database of ΔW_{ELM} values due to naturally occurring ELMs in several existing tokamaks, it is found that:

$$\Delta W_{\text{ELM}} = 0.2 W_{\text{plasma}} \left(\frac{\tau_{\text{ELM}}}{\tau_E} \right) , \quad (1)$$

where τ_{ELM} is the period of the ELM cycle and τ_E is the energy confinement time in plasmas with a stored energy W_{plasma} [48]. Using Eq. (1) with $W_{\text{plasma}} = 300 \text{ MJ}$ and $\tau_E = 3 \text{ s}$ i.e., $\Delta W_{\text{ELM}} = 20 \text{ MJ}$, implies that $\tau_{\text{ELM}} = 1/f_{\text{N_ELM}}$ must be reduced from $\sim 500\text{--}1000 \text{ ms}$ to approximately $15\text{--}30 \text{ ms}$ (i.e., $f_{\text{ELM}} \sim 30\text{--}60 \text{ Hz}$) in order to match $\Delta W_{\text{ELM}} = 0.7 \text{ MJ}$ ITER requirement discussed in Sec. 2. While a factor of 5 reduction in τ_{ELM} appears to be a reasonable target for ELM mitigation in ITER, since factors of 2–5 have been obtained in recent experiments on JET and DIII-D [10,49], uncertainties in the leading coefficient used in Eq. (1) and in the scaling with τ_E need to be verified with a more comprehensive database and a basic understanding of the physics implied by this relationship.

In addition to the technological challenge of injecting D_2 pellets at a frequency of 30–60 Hz in ITER there are questions as to whether the physics of the pedestal and ELM dynamics, τ_E and the pellet ablation physics will remain invariant as τ_{ELM} is reduced from 100 ms to 15 ms in burning plasmas with $T_e^{\text{ped}} = 5.0 \text{ keV}$.

A detailed physics understanding is being assembled using numerical models of the instability driven by the local pressure perturbation triggered by the pellets. Based on recent simulations using the nonlinear JOREK MHD code [50], which solves a set of reduced MHD equations in a toroidal geometry with both open and closed field lines, ELM pellets produce a large density perturbation that expands at the local sound speed along the magnetic field lines [50]. Here, the pressure inside the expanding plasmoid is expected to drive the MHD instability that triggers the ELM, assuming the balance between the parallel heat conduction and the cooling rate due to the local particle source

can be maintained via the assumption of an essentially infinite parallel heat conductivity required in the model. Various uncertainties related to the requirements on the pellet size, penetration depth and particle throughput need to be resolved before a detailed design of the system based on this approach can be completed for ITER. While numerical simulations, such as those from the JOREK code, are vital for scaling this concept to ITER, additional experiments are essential for developing high-repetition rate pellet injectors and for validating the physics models used in the MHD codes.

Recent experiments on DIII-D have produced promising new results on the ability to significantly reduce τ_{ELM} while maintaining relatively good values of τ_E [49]. Figure 3 shows an example of a discharge in which a series of 1.8 mm D_2 pellets, containing 2×10^{20} atoms per pellet, were injected into a DIII-D H-mode plasma with a natural ELM frequency of 5 Hz. The pellet injector in this case was triggered at 14 Hz and the resulting ELMs had a frequency of 25 Hz i.e., a factor of 5 increase in $f_{\text{N_ELM}}$ over the reference discharge. Here, the natural ELMs had an average $\Delta W_{\text{ELM}} = 85 \text{ kJ}$ while the pellet driven ELMs had an average $\Delta W_{\text{ELM}} = 22 \text{ kJ}$ with τ_E reduced by about 10% during the period with the pellet paced ELMs. It was also found that the toroidal rotation velocity at the top of the pedestal was reduced from 55 km/s without pellet pacing to 35 km/s during pellet pacing. This effect on the toroidal momentum is an area that needs to be understood since in ITER the torque from NBI heating will be relatively low implying a naturally low toroidal velocity without pellet pacing. It needs to be understood whether this reduction in the toroidal rotation is an intrinsic effect of the increased ELM frequency or an enhancement in toroidal momentum transport due to an increase in the neutral particle density from the pellets. In either case, this could be a significant issue for avoiding field-error penetration and mode locking as the toroidal rotation is reduced during high frequency pellet pacing operations. In addition, the elevated neutral density in the pedestal region could significantly enhance the charge exchange rate between the

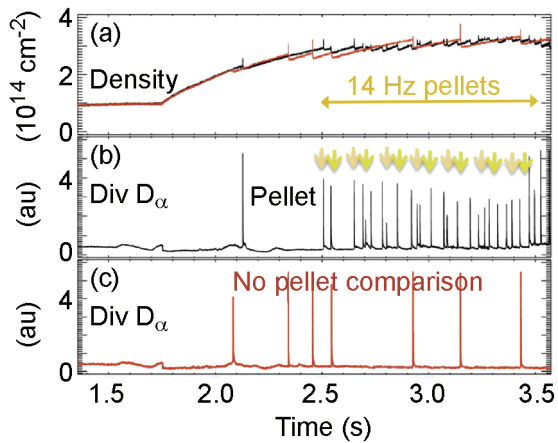


Fig. 3. ELM response to 18 mm D_2 pellets injected into a DIII-D H-mode plasma. (a) Plasmas density and the time interval over which the 14 Hz pellets were injected, (b) divertor D_α recycling showing 25 Hz ELMs triggered by the pellets and (c) natural ELMs in a similar discharge with no pellets (from Baylor, *et al.*, Ref. 49).

neutrals in the pellet cloud and hot plasma ions in the pedestal causing a loss of momentum, particle and energy confinement and adding a source of fast neutral flux to the main chamber walls. Finally, it is necessary to determine the minimum pellet size needed to trigger ELMs since the particle throughput for pellet pacing must be minimized in ITER. Overall, the pellet pacing approach looks promising but a significant level of numerical modeling and experimentation on existing tokamaks is still required to establish a detailed physics understanding of the requirements needed to design an efficient and reliable system for ITER.

4. ELM SUPPRESSION AND MITIGATION USING RMP FIELDS

A long history of experiments have demonstrated that intrinsic and applied non-axisymmetric magnetic fields, generally referred to as RMP fields, provide a very effective mechanism for controlling the macroscopic dynamics of the plasma in tokamaks and stellarators. These experiments have shown that plasmas exposed to low-level RMP fields are quite sensitive to relatively small changes in the external parameters of the control fields, a well known property of a complex nonlinear dynamical system [51], and can display a rich spectrum of dynamical behaviors. For example, it has recently been demonstrated, in a variety of tokamaks [4–8, 52–54] and stellarators [55], that small RMP fields can be used to control the pedestal plasma in H-modes in such a way as to completely suppress or mitigate ELMs. A recent comprehensive summary of RMP ELM control experimental results and machine specific hardware on all the tokamaks that are currently engaged in this type of research is given in Refs. 56 and 57. In addition, a review specifically focused on ELM mitigation results with RMP fields in JET can be found in Ref. 58.

Although there are a rather broad range of effects associated with the presence RMP fields in both L-mode and H-mode plasmas, the discussion here is focused on describing changes in the dynamics of the global particle balance during RMP experiments. Since significant changes in the plasma density, turbulence and neutral particle dynamics stand out as one of the most prevalent effects of the RMP fields observed in most experiments, this is a topic of fundamental interest for understanding the physics of RMP interactions with the plasma and provides a good focal point for a limited review of RMP ELM mitigations and suppression such as the one given in this paper.

Starting with the first RMP experiments on the TEXT, it was realized that the ability to modify the exchange of neutrals and ions between the plasma facing components and the edge plasma was a very effective way of controlling the performance of the tokamak [59–61]. These early experiments paved the way for extensive studies of the so-called “density pump-out” effect and the discovery of RMP improved confinement regimes without ELMs in the JIPP T-IIU [62], Tore Supra [51,63], COMPASS-C [64] and TEXTOR [65] tokamaks as well as in the Wendelstein 7-AS stellarator [66] and the LHD helitorn [67]. Based on the TEXT, JIPP T-IIU and Tore Supra results it was proposed that

RMP fields could be used to control ELMs [68] and several early experiments in diverted tokamaks were attempted [23,69] that resulted in the destabilization of small ELMs in naturally occurring ELM-free H-modes with an uncontrolled density rise. These first ELM control attempts defined an operational space known today as the RMP ELM mitigation regime where small high-frequency ELMs are driven by the RMP field. The discovery of full ELM suppression with RMP fields in both high density (v_e^*) [4,70] and low density (v_e^*) [5,70] DIII-D H-modes sparked a worldwide research effort to better understand the physics of RMP ELM control and the inclusion of ELM control coils inside the ITER vacuum vessel [47]. This led to a confirmation of the high-density ELM mitigations results in ASDEX-Upgrade where some of the properties seen in the original DIII-D experiments were reproduced while others were not [7]. The key to the success of this approach is the ability of the RMP field to maintain steady-state density and impurity control with either small ELMs (mitigation) or no ELMs at all (suppression) over a wide range of pedestal parameters [4,70–72].

Figure 4 shows two examples of high-density (v_e^*) ELM suppression in DIII-D [4,70]. Here, the response to an equivalent RMP (I-coil) pulse is shown in plasmas with slightly different shapes. It is seen that the line average density n_e is not significantly reduced during the RMP phase in either of these high-density discharges and although there is a slight increase in Z_{eff} there is no significant change in τ_E , the H factor or W_{plasma} in either of these plasmas except after 3400 ms in 115467 when there was a switch from the 150R neutral beam to the 30L neutral beam resulting in the small drop in n_e seen in Fig. 4(a). A significant difference in these two discharges, other than an increase in the lower triangularity $\delta_L = 0.601$ in 119690 to $\delta_L = 0.728$ in 115467, is an increase in the neutral particle recycling with a much lower gas fueling rate during 119690 compared to that during 115467. This highlights the importance of understanding the neutral particle dynamics i.e., particle sources and sinks during RMP ELM control experiments and the effects of changing wall conditions.

Detailed studies of the global particle balance in discharges similar to those seen in Fig. 4 have shown that the effective particle confinement time ($\tau_p^* = \tau_p / (1 - R)$ where R is the recycling coefficient) increases with increasing v_e^* [73]. It has also been shown that there is a substantial increase in pedestal density fluctuations [74] in these high-density (v_e^*) ELM suppression discharges. It is conceivable that the interaction of the higher neutral density with the pedestal plasma increases the turbulence and changes the dynamics to a more bursty or intermittent type of transport that is typical of high v_e^*

H-modes with naturally small ELMs. Thus, under this scenario the energy need to drive large Type-I ELMs is dissipated by an increase in the intermittent transport driven by higher neutral densities and recycling.

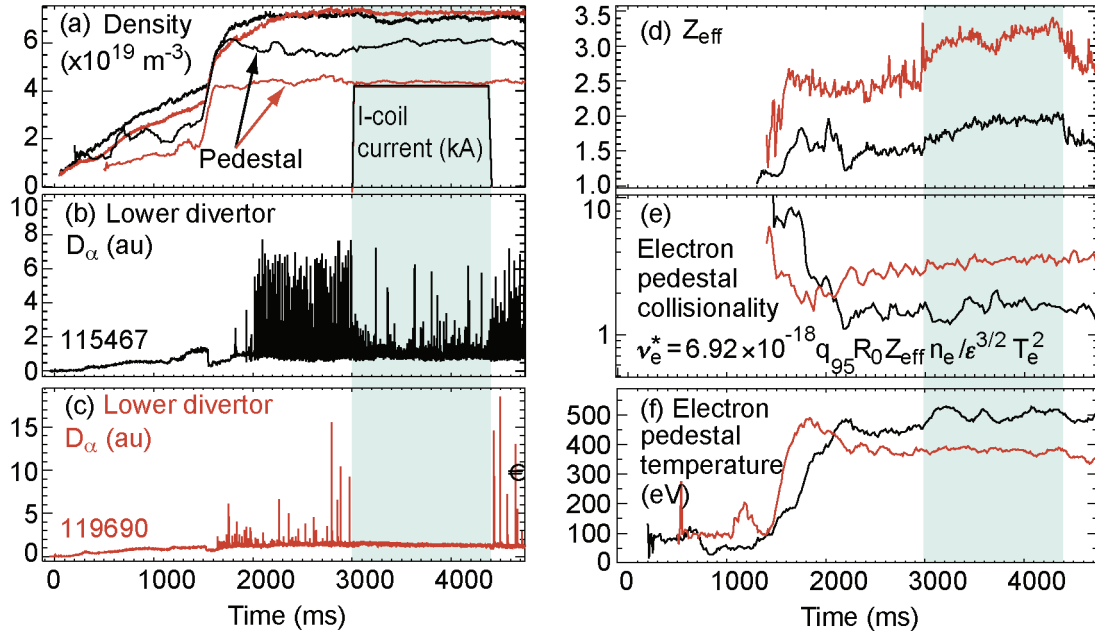


Fig. 4. Comparison of RMP plasma response in two similar DIII-D plasmas with slightly different shapes where (a) the pedestal and line average density, (b) the divertor recycling in 115467, (c) the divertor recycling in 119690, (d) the edge Z_{eff} , (e) the electron pedestal ν_e^* and (f) the electron pedestal temperature are seen to be quite different from the beginning of the discharges.

In low collisionality discharges, with $\nu_e^* = 0.1 - 0.04$, full ELM suppression is reproducibly obtained over a wide range of pedestal and core confinement regimes in DIII-D but it is also found that the response, particularly that of the pedestal density and neutral particle dynamics, is quite sensitive to δ_L and the geometry of the divertor as discussed in Refs. 70, 71 and 75–77. In general, ITER similar shaped plasmas with $\delta_L = 0.70$ and a somewhat more closed divertor geometry require higher RMP fields to obtain ELM suppression than plasmas with $\delta_L = 0.37$ and an open divertor geometry. Detailed particle balance studies in these two cases show that the neutral particle recycling is an important player in the significantly different density response and confinement changes seen in these two cases [76].

In lower single null plasmas with a lower triangularity $\delta_L = 0.37$ and a relatively open divertor configuration, changes in the pedestal and core density result in an interesting operating regime with properties that look somewhat similar to those observed in plasma

with internal ion transport barriers [71]. Figure 5 shows the evolution of the line-averaged density and the pedestal density before and during the application of the RMP field from the DIII-D I-coil. As seen in Fig. 5(a), during the initial part of the I-coil phase the line-average density is essentially constant while the pedestal density drops immediately when the RMP fields are applied. Before applying the RMP field, during the period with large Type-I ELMs, the density peaking factor n_e^0/n_e^{ped} varies between 0.8 and 1.1 but during the early I-coil phase, prior to $t = 2.0$ s, n_e^0/n_e^{ped} stabilizes at 1.2. Figure 5(b) shows the evolution of the ELMs as q_{95} approaches the resonant window for full ELM suppression. The ELMs are initially mitigate by the RMP field, while $q_{95} > 3.7$, and then fully suppressed after $t = 2.1$ s once $q_{95} = 3.7$ i.e.,

the upper boundary of the ELM suppression resonant window. Here the peaking factor increases to 1.4 and then both the line-average and pedestal density drop at approximately the same rate to a new steady-state level that is maintained until the end of the I-coil phase. See Ref. 71 for more details on this discharge and comparisons with ELM suppression in higher δ_L ITER Similar Shaped plasma. Recent experiments indicate that the reduction in the line-average and pedestal density can be minimized or essentially eliminated by adjusting the I-coil current once ELM suppression is obtained [78]. This illustrates the need for active feedback control of the RMP field in order to simultaneously optimize ELM suppression and the plasma performance. Figure 6 shows the density profiles averaged over

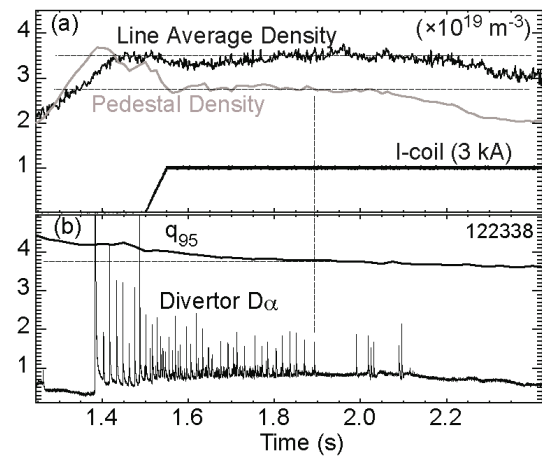


Fig. 5. Evolution of the line-average and pedestal density versus time before and during the application of the RMP filed from the DIII-D I-coil (a) and the change in ELMs due to the RMP field as q_{95} crosses the upper boundary of resonant window for full ELM suppression located at $q_{95} = 3.7$.

the upper boundary of the ELM suppression resonant window. Here the peaking factor increases to 1.4 and then both the line-average and pedestal density drop at approximately

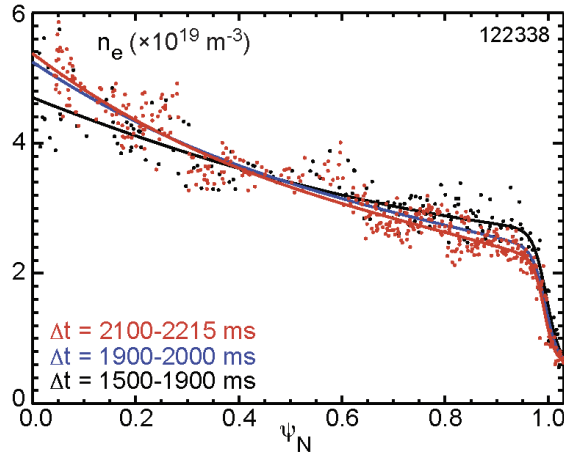


Fig. 6. Changes in the electron density profile measured with a Thomson scattering system on DIII-D before the introduction of an $n = 3$ RMP field averaged over $t = 1500-1900$ ms (black), during the ELM mitigated phase of the RMP pulse $t = 1900-2000$ ms (blue) and the ELM suppressed phase of the RMP pulse $t = 2100-2215$ ms (red) for the discharge shown in Fig. 5.

three time windows for the discharge shown in Fig. 5. Here we see that the RMP field reduces the pedestal density and increases the core density which may be an acceptable solution for $Q_{DT} = 10$ operations in ITER based on the TGLF-09 results discussed above. Dedicated TGLF-09 simulations are needed to assess this hypothesis.

An important attribute of the RMP ELM control approach is the ability to adjust the properties of the perturbation field for different plasma shapes and operating conditions. This has made it possible to obtain ELM mitigation or suppression in every operating scenario normally encountered in DIII-D. In ITER the ELM coils are designed to provide complete control over the amplitude and phase of the perturbation field. This is important for implementing real-time feedback control algorithms to compensate for changing plasma, divertor and wall conditions. In addition, the ITER RMP fields will be rotated toroidally at up to 5 Hz to smooth out the steady-state divertor heat flux during ELM suppression or mitigation [47].

5. SUMMARY AND CONCLUSIONS

Current estimates of the erosion rate of tungsten divertor target plates in ITER indicate that the energy incident on the surface of the divertor due to each ELM (ΔW_{ELM}) must be reduced from 20–30 MJ to approximately 0.7 MJ (0.5 MJ m^{-2}) assuming an impulse deposition time $\Delta t_{\text{ELM}} \geq 250\text{--}500 \mu\text{s}$ [47]. There are significant uncertainties in these estimates due to inherent nonlinearities in the heat and particle interaction models being used, the material (tungsten) properties of target plates when exposed to the extreme conditions expected in the ITER divertor and the scaling of the deposition area with ELM size. The best estimates of the damage that can be expected due impulsive loading from large ELMs are derived from laboratory experiments using a plasma accelerator to generate intense heat pulses that interact with ITER-like material [45,46]. While these have provided important information on the response of various materials to high heat pulses, they do not fully account for the conditions that will be present in the ITER divertor during high-recycling operations with impurity seeding or the long term effects of changes in the plasma facing components in the ITER divertor environment.

A wide variety of potentially useful ELM mitigation systems are actively being developed, as discussed in Sec. I, but the requirements for ELM control in ITER are extremely stringent and none of these systems have demonstrated the ability to meet all the requirements simultaneously in today’s tokamaks where the pedestal conditions are well removed from those that will be encountered in ITER. More importantly, since it is not possible to reproduce the ITER pedestal conditions in today’s tokamaks, i.e., $n_e^{\text{ped}} = 9 \times 10^{19} \text{ m}^{-3}$ with $v_e^* = 0.1\text{--}0.03$, it is essential to understand the basic physics involved in any approach under consideration since it is necessary to determine whether the system will scale to the ITER pedestal conditions and do so without significantly degrading the pedestal confinement or core stability of the plasmas required to achieve $Q_{\text{DT}} = 10$.

Although, the current ITER baseline ELM control systems, i.e., pellet pacing and RMP fields, are presently the most promising and well developed of all the techniques being considered, in terms of meeting all the ITER requirements discussed in Sec. II, there are considerable gaps in the physics basis needed to scale these systems to a

burning plasma regime and, additionally, neither system has proven that it can simultaneously satisfy all the ITER requirements in today's tokamaks. With this in mind, and knowing the importance of ELM control in ITER as well as in the next generation of ignited plasmas beyond ITER, it is obvious that ELM control is an area of research that needs to be supported at the highest possible level in order to ensure the successful realization of a practical magnetic fusion energy device in the near future.

REFERENCES

- [1] M. Shimada, *et al.*, Nucl. Fusion **47** (2007) S1.
- [2] A. Loarte, *et al.*, Plasma Phys. Control. Fusion **45** (2003) 1549.
- [3] J.E. Kinsey, *et al.*, Nucl. Fusion **51** (2011) 083001.
- [4] T.E. Evans, *et al.*, Phys. Rev. Lett. **92** (2004) 235003.
- [5] T.E. Evans, *et al.*, Nature Phys. **2** (2006) 419.
- [6] Y. Liang, *et al.*, Phys. Rev. Lett. **98** (2007) 265004.
- [7] W. Suttrop, *et al.*, Phys. Rev. Lett. **106** (2011) 225004.
- [8] Y. M. Jeon, *et al.*, submitted to Phys. Rev. Lett. (2012).
- [9] P.T. Lang, *et al.*, Nucl. Fusion **43** (2003) 1110.
- [10] P.T. Lang, *et al.*, Nucl. Fusion **51** (2011) 033010.
- [11] L.R. Baylor, *et al.*, Bull. Am. Phys. Soc. **51** (2006) 115.
- [12] K.H. Burrell, *et al.*, Plasma Phys. Control. Fusion **44** (2002) A253.
- [13] K.H. Burrell, *et al.*, Phys. Plasmas **12** (2005) 056121.
- [13] A.M. Garofalo, *et al.*, Nucl. Fusion **51**, 083018 (2011).
- [14] W. Suttrop, *et al.*, Plasma Phys. Control. Fusion **45**, 1399 (2003).
- [15] Y. Sakamoto, *et al.*, Plasma Phys. Control. Fusion **46**, A299 (2004).
- [16] W. Suttrop, *et al.*, Nucl. Fusion **45**, 721 (2005).
- [17] F. Ryter, *et al.*, Plasma Phys. Control. Fusion **40** (1998) 725.
- [18] R.M. McDermott, *et al.*, Phys. Plasmas **16**, 056301 (2009).
- [19] D.G. Whyte, *et al.*, Nucl. Fusion **50** (2010) 105005.
- [20] S. Jachmich, *et al.*, J. Nucl. Mater. **415** (2011) S894.
- [21] J. Rapp, *et al.*, Plasma Phys. Control. Fusion **44** (2002) 639.
- [22] Y. Corre, *et al.*, Plasma Phys. Control. Fusion **50** (2008) 115012.
- [23] S.J. Fielding, *et al.*, Proc. 28th EPS Conf. on Controlled Fusion and Plasma Phys. (Madeira), ECA, Vol. **25A** (2001) p. 1825.
- [24] A.W. Degeling, *et al.*, Plasma Phys. Control. Fusion **45** (2003) 1637.
- [25] Y. Martin, *et al.*, Proc. 31st EPS Conf. on Controlled Fusion and Plasma Phys. (London), ECA, Vol. **28G** (2004) P4-133.
- [26] T. Rhee, *et al.*, Phys. Plasmas **19** (2012) 022505.
- [27] W.W. Xiao, *et al.*, “ELM mitigation by supersonic molecular beam injection into the H-mode pedestal in HL-2A tokamak,” submitted to Nucl. Fusion (2012).

- [28] J. Kim, *et al.*, “ELM control experiments in the KSTAR device,” submitted to Nucl. Fusion (2012).
- [29] R. Maingi, *et al.*, Phys. Rev. Lett. **103** (2009) 075001.
- [30] R. Maingi, *et al.*, submitted to Nucl. Fusion (2012).
- [31] H.W. Kugel, *et al.*, J. Nucl. Mater. **415** (2011) S400.
- [32] J.X. Rossel, *et al.*, Nucl. Fusion **52** (2012) 032004.
- [33] H. Urano, *et al.*, Nucl. Fusion **47** 706.
- [34] G. Saibene, *et al.*, 2007 Nucl. Fusion **47** 969.
- [35] J.L. Terry, *et al.*, Nucl. Fusion **45** (2005) 1321.
- [36] Y. Kamada, *et al.*, Plasma Phys. Control. Fusion **42** (2000) A247.
- [37] G. Saibene, *et al.*, Nucl. Fusion **45** (2005) 297.
- [38] K. Kamiya, *et al.*, Phys. Plasmas **13** (2006) 032507.
- [39] T. Ozeki, *et al.*, Nucl. Fusion **30** (1990) 1425.
- [40] R. Maingi, *et al.*, Nucl. Fusion **45** (2005) 264.
- [41] F. Piras, *et al.*, Plasma Phys. Control. Fusion **52** (2010) 124010.
- [42] N. Oyama, *et al.*, Plasma Phys. Controlled Fusion **48** (2006) A171.
- [43] D.D. Ryutov, *et al.*, Phys. Plasmas **14** (2007) 064502.
- [44] G. Federici, *et al.*, Plasma Phys. Control. Fusion **45** (2003) 1523.
- [45] A. Zhitlukhin, *et al.*, J. Nucl. Mater. **363–365** (2007) 301.
- [46] N. Klimov, *et al.*, J. Nucl. Mater. **390–391** (2009) 721.
- [47] A. Loarte, *et al.*, Proc. 23rd IAEA Fusion Energy Conf. (Korea, 2010) ITR/1-4.
- [48] A. Herrmann, *et al.*, Plasma Phys. Control. Fusion **44** (2002) 883.
- [49] L.R. Baylor, *et al.*, Proc. 37th EPS Conf. on Plasma Phys. (Dublin) (2010) P2.117.
- [50] G.T.A. Huysmans, Proc. 37th EPS Conf. on Plasma Phys. (Dublin, 2010) P4.132.
- [51] T.E. Evans, in *Chaos, Complexity and Transport: Theory and Applications*, Ed. Cristel Chandre, Xavier Leoncini and George Zaslavsky, World Scientific Press (2008) 147–176.
- [52] A. Kirk, *et al.*, Proc. 23rd IAEA Fusion Energy Conf. (Korea, 2010) EXD/8-2.
- [53] A. Kirk, *et al.*, Nucl. Fusion **50** (2010) 034008.
- [54] O. Schmitz, *et al.*, Plasma Phys. Control. Fusion **50** (2008) 124029.
- [55] K. Toi, personal communication (2012).
- [56] M.E. Fenstermacher, *et al.*, Proc. 23rd IAEA Fusion Energy Conf. (Korea, 2010) ITR/P1-30.
- [57] N. Oyama, J. Physics: Conference Series **123** (2008) 012002.
- [58] Y. Liang, *et al.*, Plasma and Fusion Research **5** (2010) S2018.
- [59] T.E. Evans, *et al.*, J. Nucl. Mater. **145–147** (1987) 812.

- [60] N. Ohyabu, *et al.*, J. Nucl. Mater. **145–147** (1987) 844.
- [61] S.C. McCool, *et al.*, Nucl. Fusion **30** (1990) 167.
- [62] T.E. Evans, *et al.*, J. Nucl. Mater. **162–164** (1989) 636.
- [63] T.E. Evans, *et al.*, J. Nucl. Mater. **196–198** (1992) 421.
- [64] T.C. Hender, *et al.*, Nucl. Fusion **32** (1992) 2091.
- [65] K.H. Finken, *et al.*, Phys. Rev. Lett. **98**, 065001 (2007).
- [66] K. McCormick, *et al.*, J. Nucl. Mater. **313–316** (2003) 1131.
- [67] T. Morisaki, *et al.*, Fusion Science Technol. **58** (2010) 232.
- [68] T.E. Evans, *et al.*, Max-Planck Institut für Plasmaphysik Report IPP III/154 (1991).
- [69] T. Shoji, *et al.*, J. Nucl. Mater. **196–198** (1992) 296.
- [70] T.E. Evans, *et al.*, Nucl. Fusion **45** (2005) 595.
- [71] T.E. Evans, *et al.*, Nucl. Fusion **48** (2008) 024002.
- [72] M.E. Fenstermacher, *et al.*, Phys. Plasmas **15** (2008) 056122
- [73] E.A. Unterberg, *et al.*, J. Nucl. Mater. **390–391** (2009) 486.
- [74] R.A. Moyer, *et al.*, Phys. Plasmas **12** (2005) 056119
- [75] T.E. Evans, *et al.*, Phys. Plasmas **13** (2006) 056121
- [76] E.A. Unterberg, *et al.*, Nucl. Fusion **49** (2009) 092001.
- [77] K.H. Burrell, *et al.*, Plasma Phys. Control. Fusion **47** (2005) B37.
- [78] T.E. Evans, *et al.*, Bull. Am. Phys. Soc. **56** (2011) 293.

ACKNOWLEDGMENT

This work was supported by the US Department of Energy under DE-FC02-04ER54698.